Wave block formation in homogeneous excitable media following premature excitations: Dependence on restitution relations

Philippe Comtois,[1,*] Alain Vinet,[2] and Stanley Nattel[3]
[1]*Department of Pharmacology, McGill University, Montreal (Quebec), Canada*
[2]*Department of Physiology and Institute of Biomedical Engineering, Université de Montréal, Montreal (Quebec), Canada*
[3]*Department of Medicine, Université de Montréal, Montreal (Quebec), Canada*
(Received 17 February 2005; revised manuscript received 23 June 2005; published 30 September 2005)

Spiral wave formation and disorganized activity in excitable media require the existence of broken waves and are related to partial wave block. The determinants of wave block in excitable systems are incompletely understood, especially for cardiac excitable tissue. Previous work in one-dimensional cardiac models has suggested that wave break of a premature excitation (PE) requires critical timing and that the conditions for broken waves are improbable. We analyzed the mechanism of unidirectional wave block that occurs when two consecutive PEs interact with a normal plane wave in a generic one-dimensional spatial excitable medium. A nondimensional coupled-map model built from mesoscopic characteristics of the substrate (the velocity and action potential duration restitution functions) shows that block can occur over a large interval of timing between the two PEs and leads to wave break in two-dimensional media. This mechanism may be an important determinant of spiral wave formation by the response to premature excitations.

DOI: 10.1103/PhysRevE.72.031919 PACS number(s): 87.19.Hh, 05.45.−a

In excitable media, single or multiple spiral waves can be initiated by wave break [1,2], which occurs when propagation is blocked along some portion of an excitation front [3]. This phenomenon is particularly relevant to cardiac excitable tissue that can sustain the propagation of a single rotor [4] or numerous spiral waves [5], which can then lead to potentially serious cardiac arrhythmias such as fibrillation [6]. A broken wave can be induced by a stimulus applied in the vulnerable window of a portion of the tissue lying at the border of a region that is still unexcitable [7]. However, the relevance of this mechanism to the formation of cardiac arrhythmia can be questioned since, in homogeneous one-dimensional (1D) models, the range of stimulus timing associated with the vulnerable window lasts for at most a few milliseconds [8]. Alternative mechanisms of wave block involving the application of multiple local stimuli have been proposed, such as the formation of spatial oscillations in the duration of the refractory period (alternans) induced by an acceleration of the stimulation frequency [9–11], or the induction of discordant alternans with a limited number of stimuli [10]. It is generally assumed that partial wave block following a limited number of premature excitations in real cardiac tissue depends on the presence of structural and/or cellular heterogeneities. Nevertheless, some experiments have clearly shown an increase vulnerability to arrhythmias following a single premature activation [12]. These results are consistent with a new scenario of unidirectional block described in a model of a homogeneous cardiac tissue that involves the interaction of a preexisting wavefront with only two premature stimuli [13] and experimental data obtained in canine hearts [14]. In this paper, we provide a description of this mechanism of unidirectional block in a generic model of 1D excitable medium. A coupled-map model based on mesoscopic characteristics of the substrate (functions describing the restitution of velocity of propagation and of the duration of the action potential) shows that the block can occur for a large interval of timing between the two premature excitations. We also show that this new mechanism of block can lead to wave break and to the formation of a spiral wave in a two-dimensional (2D) medium.

I. MODEL

The model follows from an integral-delay formulation that was proposed to describe reentry in a one-dimensional ring [13,15]. Consider the propagation of successive activation fronts in a 1D cable of length L. The passage of the nth activation front at one location is characterized by $T_{\mathrm{act},n}(x)$, the activation time, and $T_{\mathrm{rep},n}(x)$, the time at which the post-activation unexcitable period (refractory period) ends. The next activation occurs at a recovery time given by $\delta_{n+1}(x) = T_{\mathrm{act},n+1}(x) - T_{\mathrm{rep},n}(x)$ which represents the time elapsed since the end of the last action potential. The model assumes that the intrinsic duration of the action potential would be a simple function of δ if the site were disconnected from its neighbors, such that $T_{\mathrm{rep},n}(x)$ would be $T_{\mathrm{act},n}(x) + a(\delta_n(x))$, in which $a(\delta)$ is the action potential restitution function. However, the resistive coupling between cells generates a diffusion current that reduces the spatial gradient in action potentials duration and in T_{rep}. This smoothing effect of the diffusion current is introduced by taking a weighted average of $T_{\mathrm{rep},n}$ over a neighborhood α, such that $T_{\mathrm{rep},n}(x) = \int_{x-\alpha}^{x+\alpha} \omega(y)\{T_{\mathrm{act},n}(y) + a[\delta_n(y)]\}dy$, with $\alpha = 0.005$ normalized units (n.u., see below) and $\omega(x) = N^{-1}\exp(-\beta x^2)$ ($\beta = 3.2 \times 10^5$ (n.u.)$^{-2}$ and N is the normalization coefficient) [16–18].

The speed of propagation θ is also assumed to be a function of δ. Accordingly, in the case of a wave front propagat-

*Electronic address: p-comtois@crhsc.rtss.qc.ca

ing from x_1 to x_2 in the positive direction, δ of the $n+1$ activation is given by

$$\delta_{n+1}(x_2) = T_{\mathrm{act},n+1}(x_1) + \int_{x_1}^{x_2} \frac{dk}{\theta(\delta_{n+1}(k))} - T_{\mathrm{rep},n}(x_2). \quad (1)$$

In this study, the model is made nondimensional by dividing the time by $(\mathrm{APD})_{\max}$, the maximum value of the action potential duration, and the space by $(\mathrm{APD})_{\max} \times \theta_{\max}$, where $\theta_{\max}$ is the maximum value of propagation speed. The nondimensional Eq. (1) is analyzed with the dispersion and restitution functions

$$\xi(\delta) = 1 - \gamma_\xi e^{-\delta/\tau_\xi} \quad \text{for} \quad \xi \in \{\theta, a\} \quad \text{and} \quad \delta \geqslant 0. \quad (2)$$

Each of these functions is thus characterized by two parameters: the minimum value $1-\gamma_\xi$ and the rate of variation $1/\tau_\xi$. Hereafter, the first (P_1) and second (P_2) premature activations are both initiated in the middle of the cable ($x_{\mathrm{PE}} = L/2$) after the passage of a normal wave, corresponding to a wavefront traveling from the left end to the right end of the cable. The normal wave thus propagates at $\theta_{\max}$ (=1 in n.u.) and produces an action potential of duration $(\mathrm{APD})_{\max}$ (=1 in n.u.). The time of the passage of the normal wave at x_{PE} is taken as a reference (i.e., $t=0$) to study the effect of the premature activations P_1 and P_2.

The interaction between a plane wave and two premature activations is also studied by numerical simulation of a 2D homogeneous and continuous sheet model with Neumann boundary conditions. Equation (3) [19] is solved for the transmembrane potential V, in which the reaction term $g(V,\vec{z})$ is represented by the Fenton-Karma equations [20] (parameters are set as in Ref. 18) and I is the stimulus current (to activate premature activations)

$$\partial_t V = D\nabla^2 V - g(V,\vec{z}) - I, \quad \partial_t \vec{z} = \vec{F}(V,\vec{z}). \quad (3)$$

The Fenton-Karma model was chosen because it is low dimensional and because its parameters can be easily adjusted to obtain different action potential and velocity restitution functions.

II. FROM SYMMETRIC TO ASYMMETRIC DYNAMIC HETEROGENEITIES

Numerical solution of Eq. (1) shows that, following the normal wave (bottom thick continuous curve in all panels of Fig. 1), a first premature activation P_1 (second thick continuous curve) applied beyond the unexcitable period (gray area) results in bidirectional propagation (R_1, activation front in the retrograde direction and A_1, front in the antegrade direction). The profile of T_{rep} depends on the timing of the P_1 and on the characteristics of the restitution functions. A late P_1 creates a symmetric profile of T_{rep} around x_{PE}, as shown in Fig. 1(a) (upper dashed line). A more premature P_1 (decreasing the time between the normal wave and P_1) spawns an asymmetric profile of T_{rep} [Fig. 1(b), upper dashed curve]. The asymmetry in T_{rep} reflects the asymmetry of δ around x_{PE} which controls the action potential duration and the velocity of propagation. The sharp increase of δ in the retrograde direction induces a steep prolongation of the action potential duration [through $a(\delta)$]. In the antegrade direction, the small δ values slow the propagation, and act upon T_{rep} by delaying the time of activation. Figure 1(c) shows that the profile of T_{rep} is crucial to the behavior of the second stimulation P_2. The retrograde front R_2 can block in the reverse direction under conditions that allow A_2 to propagate. Hereafter only a single timing for P_1 will be studied corresponding to the most premature activation creating bidirectional propagation as in Fig. 1(b).

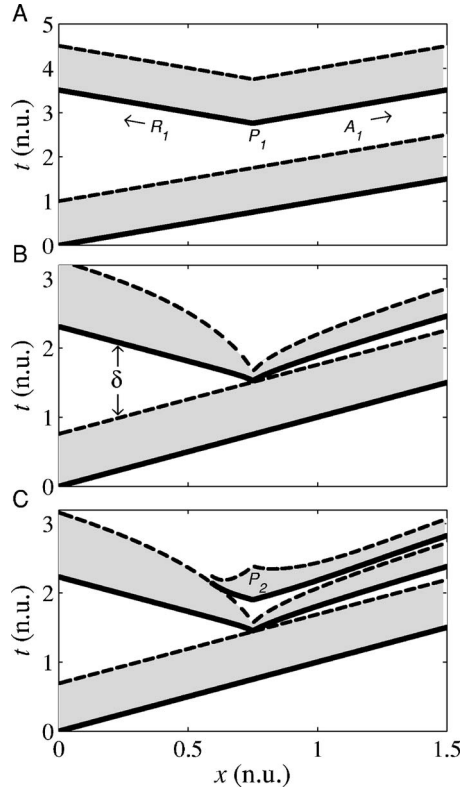

FIG. 1. Numerical integration of Eq. (1) with a regular wave propagating from $x=0$ [$T_{\mathrm{act}}(x)$, bottom thick continuous curve with inexcitable period of the substrate in gray and $T_{\mathrm{rep}}(x)$, dashed curve]. The variables t and x are in normalized units (n.u.). (a) A late premature activation (P_1) at $x=0.75$ induces propagation on both side of the initiating point. Note that T_{rep} is symmetric around $x=0.75$. (b). Similar to panel (a) but for a more premature activation showing the formation of an asymmetric profile of T_{rep}. (c). A second premature activation (P_2) at $x=0.75$ following the same first PE as in (b), creates two fronts, of which only one is sustained.

A. Time interval for retrograde block

Equation (1) is solved for the most premature P_1 and the time interval between P_1 and P_2 is then scanned for a set of $\{\tau_\theta, \tau_a\}$ with fixed $\{\gamma_\theta, \gamma_a\}$. The criteria for the most premature P_1 is that it is the smallest coupling that induces bidirectional propagation of A_1 and R_1 around x_{PE}, as in Fig. 1(b). Figure 2(a) shows $\Delta_{b,R2}$, the width of the coupling interval between P_1 and P_2 leading to bidirectional propagation at x_{PE}, followed by a block of R_2 at some distance from the activation site. This interval begins immediately after the

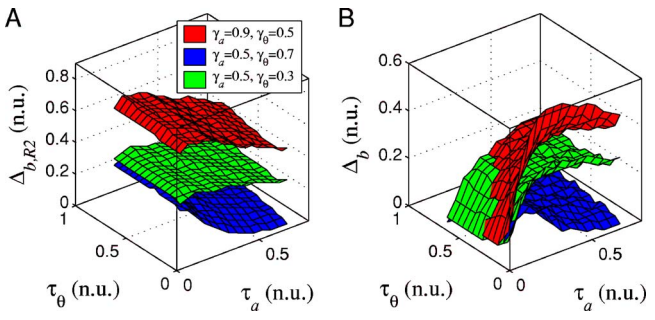

FIG. 2. (Color online) (a) The interval of retrograde block ($\Delta_{b,R2}$) in normalized units (n.u.) varies with τ_θ and τ_a of the restitution relations (shown for three sets of γ, see legend for details). (b) The interval of unidirectional block (Δ_b) corresponding to block of R_2 while A_2 propagates in the antegrade direction differs from (a) because A_2 blocks with R_2 for small τ_a. For comparison purpose, unidirectional block with a single PE exists over a time interval of 1.9×10^{-3}.

end of the unexcitable period associated with P_1 at x_{PE}, and ends when R_2 is no longer blocked and can propagate to reach the left end of the cable. However, R_2 being blocked does not exclude the possibility that the antegrade front A_2 can also be stopped at some distance of x_{PE}, an issue that will be discussed later.

The parameters τ_a, γ_a, and γ_θ have a major influence on $\Delta_{b,R2}$. Shorter τ_a, which implies a steeper slope for the action potential restitution function, produces longer $\Delta_{b,R2}$. Larger γ_a, implying both a steeper restitution function and a shorter minimum duration, also prolongs $\Delta_{b,R2}$. Finally, smaller γ_θ, which indicates more limited variation in velocity as a function of δ, increases $\Delta_{b,R2}$ to larger values. In order to better understand the dependence of $\Delta_{b,R2}$ on the parameters of the restitution relations, Eq. (1) is studied for the special case where τ_θ is small. In this case, the activation front propagates at maximum speed, except for very small values of δ and this allows for interesting approximations.

B. Analysis for small τ_θ

Conditions for the limit of propagation of R_2 at the point y_0 ($y=x_{\mathrm{PE}}-x$, $x\leqslant x_{\mathrm{PE}}$) can be summarized as

$$T_{\mathrm{rep},R1}(y_0) = T_{\mathrm{act},R2}(y_0), \tag{4}$$

$$\left|dT_{\mathrm{rep},R1}/dy\right|_{y=y_0} = 1/\theta_{\min} = 1/(1-\gamma_\theta). \tag{5}$$

It corresponds to the collision of the activation front R_2 with the refractory tail left by R_1 ($T_{\mathrm{rep},R1}$) at the minimum speed $\theta_{\min}$. Neglecting the effect of coupling on the repolarization time simplifies Eq. (1) to $T_{\mathrm{rep},n}(y)=T_{\mathrm{act},n}(y)+a(\delta_n(y))$, which is the original formulation proposed by Refs. 21 and 22.

Setting $t=0$ to be the end of the refractory period of the normal front at $y=0$ ($x=x_{\mathrm{PE}}$), taking δ_{P1} to be the recovery time associated the first premature excitation at $y=0$, and assuming that the normal wave and the retrograde front are propagating at maximum velocity ($\theta_{\max}=1$ in normalized units), we find that $T_{\mathrm{act},R1}(y)=\delta_{P1}+y$ and $\delta_{R1}(y)$, the recovery time encountered by $R_1=\delta_{P1}+2y$, such that

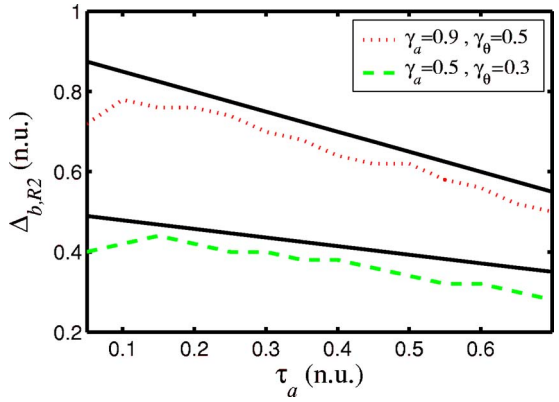

FIG. 3. (Color online) The interval of block of R_2 (τ_θ=0.05) in normalized units (n.u.) is compared to the value approximated by Eq. (8) (continuous line above each numerical data set) for two sets of γ.

$$T_{\mathrm{rep},R1}(y) \simeq T_{\mathrm{act},R1}(y) + a(\delta_{R1}(y)) = T_{\mathrm{act},R1}(y) + a(\delta_{P1}+2y). \tag{6}$$

Taking the derivative of Eq. (6) and replacing it in condition (5) yields a relation between the slope of the restitution function and the velocity dispersion function at the limit of block

$$\left.\frac{da}{d\delta}\right|_{\delta(y_0)} \simeq \frac{\gamma_\theta}{2(1-\gamma_\theta)}. \tag{7}$$

The next step is to find an approximation for $\Delta_{b,R2}$. Starting with condition (4) and assuming the front R_2 is propagating at $\theta_{\max}$ up to the position of block [23], we find that $\Delta_{b,R2}\simeq a(\delta(y_0))-a(\delta_{P1})$, where $a(\delta_{P1})$ is the duration of the refractory period produced by P_1 at x_{PE}. In the special case where $\delta_{P1}=0$, corresponding to the more premature activation of P_1, $a(0)=1-\gamma_a$. Since $a(\delta(y_0))=1-\tau_a da/d\delta|_{\delta(y_0)}$, the interval can be approximated as

$$\Delta_{b,R2} \simeq \gamma_a - \frac{\gamma_\theta}{2(1-\gamma_\theta)}\tau_a. \tag{8}$$

Equation (8) shows that the interval of block is approximately linearly scaled with respect to γ_a and τ_a, while it can be reduced sharply at high γ_θ values. The approximation also confirms the conclusion established by a qualitative analysis of Fig. 2(a) in the previous section. Results obtained by numerical integration of Eq. (1) are compared to Eq. (8) in Fig. 3. Equation (8) gives a good upper limit for $\Delta_{b,R2}$ when τ_θ =0.02 (the time constant of the velocity restitution function). A noticeable difference in the behavior can be observed for small τ_a (the time constant of the APD restitution function) that remains to be elucidated. The approximation degrades, however, when γ_θ is increased to 0.7 (not shown) by overestimating the effect of τ_a.

III. ANTEGRADE BLOCK CAN COEXIST WITH RETROGRADE BLOCK

The time interval (Δ_b) for which only the retrograde front is blocked, while the antegrade front (A_2) is able to propa-

gate until the right end of the cable, can be calculated by numerical integration of Eq. (1). An example of this behavior is presented in Fig. 1(c). In fact, Δ_b, shown in Fig. 2(b) is the most significant result since it corresponds to the vulnerable window for unidirectional block with P_2. The most important difference between Δ_b and $\Delta_{b,R2}$ occurs for low value of τ_a, for which A_2 is blocked as well as R_2. A small τ_a means a steep increase of the action potential duration as a function of δ. The refractory tail left by P_1 then increases abruptly on each side of x_{PE}, such that both A_2 and R_2 tend to block. Work is still needed to obtain an analytical estimate of the interval at which A_2 is blocked ($\Delta_{b,A2}$), and then of Δ_b, which is equal to $\Delta_{b,R2}-\Delta_{b,A2}$.

IV. FROM 1D UNIDIRECTIONAL BLOCK TO 2D PARTIAL WAVE BLOCK AND SPIRAL WAVE CREATION

In the previous section, we have shown that retrograde block can exist over large time intervals and can occur while the antegrade front created by P_2 still propagates. This effect derives from the asymmetry of the repolarization profile generated by P_1, which depends on the fact that A_1 travels in the direction of the normal wave and R_1 in the inverse direction. A premature activation (created here by applying a stimulus) following the passage of a plane wave in a 2D substrate should create a spatial profile in T_{rep} with characteristics similar to those observed in the 1D medium. Figures 4(a)–4(d) show the spatial profile of V obtained from Eq. (3). Panel (a) described the state of the system 58 ms after the application of P_1. The tail of the previous normal plane wave is still visible near the right border of the medium, while the action potential induced by P_1 has started to propagate. P_2 produces an expanding wavefront [Fig. 4(b)] that undergoes partial wave break because of retrograde block, creating a single wavetip [Fig. 4(c)] that can reenter and entrain the medium [Fig. 4(d)]. Figure 4(e) depicts the spatial profile of T_{rep} following P_1. The main characteristic of this profile is a prominent asymmetry around the site of stimulation (illustrated by the vertical dotted line originating from the stimulation site), with a greater gradient in the retrograde direction. The feature responsible for the retrograde block of propagation in the 1D case is thus also found in the 2D simulation and is responsible for partial block of propagation. This scenario of wave block and creation of a broken wave was found to occur in an interval $\Delta_b \simeq 58$ ms (i.e., ~ 0.22 n.u. in the nondimensional form) in the 2D model.

V. RELEVANCE TO ARRHYTHMIA INITIATION IN CARDIAC TISSUE

Unidirectional block by two premature excitations was first described in numerical simulation of a 1D loop based on a Beeler-Reuter-type representation of cardiac dynamics [13]. The coupled-map model, with its general representation of the restitution and dispersion functions, shows that the phenomenon is quite general and permits isolation of the factors controlling its occurrence. The slope of action potential duration restitution and the minimum action potential duration both promote the asymmetry of the repolarization

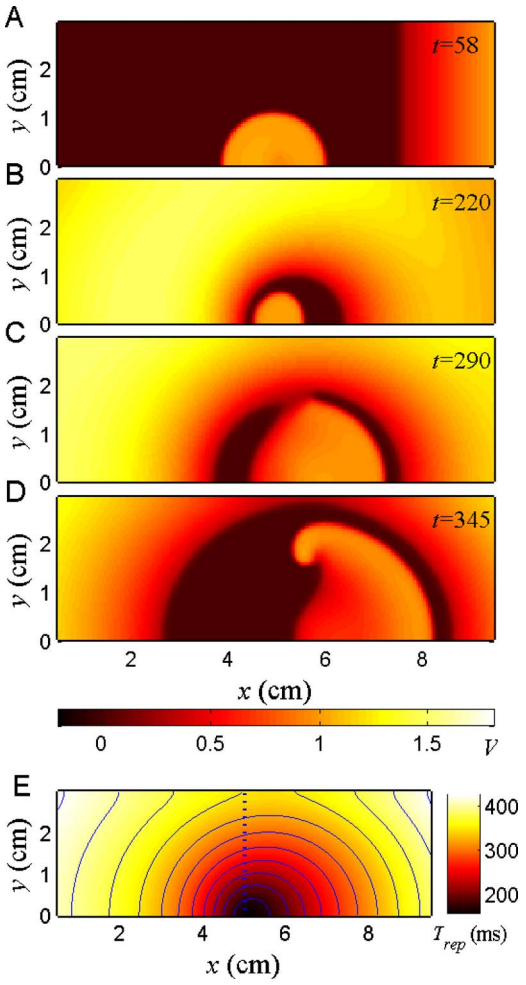

FIG. 4. (Color online) Panels (a) (d) color map of V (scale is shown below panel D) in space for the $2d$ sheet with PE at $(x_{\mathrm{PE}}, y_{\mathrm{PE}})=(5,0)$ with P_1 created 1 ms after the end of the inexcitable period. The PE are induced by localized stimuli (square pulse with $I=0.3$ for 1 ms) applied on a square subset of nodes (29 by 15 nodes). (a) The activity 58 ms after P_1. (b) P_2 appear at $t=200$ creating an outwardly propagating wave. (c) The wave first block at $y=0$ creating a wavetip near $y=1.75$. (d) The wavetip can then reenter the substrate and form a spiral wave. (e) T_{rep} of P_1 (in ms) is shown as a colormap to highlight the asymmetry along x (maximum for $y=0$) while symmetric along y.

profile associated with P_1. However, if the time constant of the APD restitution function (τ_a) becomes too small, the depression of excitability around x_{PE} becomes too deep for A_2 to propagate, thus reducing the possibility that P_2 will display unidirectional block. The other important factor is γ_θ, for which a low value favors unidirectional block. The minimum velocity of propagation (given by the nondimensional parameter $\theta_{\min}=1-\gamma_\theta$) has a strong effect on the interval of retrograde block Δ_b (under conditions associated with antegrade wave front propagation). It is clear that in the hypothetical case of $\theta_{\min}\rightarrow 0$ the interval of block will tend to zero because the retrograde front created by P_2 would be able to slow down and propagate over any gradient of unexcitability left by the previous activation. In a continuous medium, the minimum speed observed as a function of prema-

turity is always very low. However, this factor may be more crucial in a discrete structure, as in real cardiac tissue, in which cells are connected by resistive gap junctions. In principle, for real cardiac tissue as for an ionic model, obtaining τ_a, γ_a and γ_θ should allow for prediction of the range of P_1-P_2 timing that would lead to unidirectional block in a 1D medium. This could be done by solving the complete coupled-map model, or using the analytical expression given in Eq. (8). The latter is limited to cases for which $\theta(\delta)$ has a small time constant but is still relevant since it corresponds to numerous ionic models [21,24] and to experimental data [25]. In order to reconstitute the interval for specific cardiac tissues, $(\mathrm{APD})_{\max}$ is also needed. $(\mathrm{APD})_{\max}$ can be quite large as for example in human ventricular cells, for which $(\mathrm{APD})_{\max}$ is $\sim$360 ms [26]. In this case, a Δ_b=0.5 n.u. would represent 180 ms for the interval of block, which is $\sim$180 times the window of vulnerability for a single stimulus in homogeneous tissue [7].

The possibility of obtaining unidirectional block by two premature activations in a 1D model is a necessary, although nor sufficient, condition for the same process to occur in 2D conditions. Nevertheless, our simulation with the Fenton-Karma model indicates that dual premature activations in the wake of a plane wave could be a very effective way to generate reentry, with a large vulnerable window (at least for specific range of restitution characteristics). Clinical arrhythmia induction for the study of reentrant arrhythmias in man often requires the direct induction of two or more consecutive premature excitations in order to induce the clinically occurring form of reentry [27]. Early and delayed after potentials, known proarrhythmic behaviors in cardiac tissue, can generate short runs of premature beats, which may play the same role as external stimuli in creating the dynamical profile of heterogeneity. It remains to be seen if real cardiac tissues, in healthy and pathological states, display the appropriate characteristics for the phenomena demonstrated here to be important in the genesis of cardiac arrhythmias.

ACKNOWLEDGMENTS

This work was supported by a fellowship from the Natural Sciences and Engineering Research Council of Canada (P.C.). Funding support was obtained from the Canadian Institutes of Health Research and the Mathematics of Information Technology and Complex Systems (MITACS) Network of Centers of Excellence.

[1] A. T. Winfree, Science **175**, 634 (1972).
[2] A. Panfilov and P. Hogeweg, Phys. Lett. A **176**, 295 (1993).
[3] A. Karma, Phys. Rev. Lett. **71**, 1103 (1993).
[4] J. M. Davidenko *et al.*, Nature (London) **355**, 349 (1992).
[5] R. A. Gray, A. M. Pertsov, and J. Jalife, Nature (London) **392**, 75 (1998).
[6] G. K. Moe, W. C. Rheinboldt, and J. A. Abildskov, Am. Heart J. **67**, 200 (1964).
[7] A. T. Winfree, J. Theor. Biol. **138**, 353 (1989).
[8] C. F. Starmer *et al.*, Biophys. J. **65**, 1775 (1993).
[9] J. J. Fox, R. F. Gilmour, Jr., and E. Bodenschatz, Phys. Rev. Lett. **89**, 198101 (2002).
[10] J. J. Fox, M. L. Riccio, P. Drury, A. Werthman, and R. F. Gilmour, Jr., New J. Phys. **5**, 101.1 (2003).
[11] H. M. Hastings *et al.*, Phys. Rev. E **62**, 4043 (2000).
[12] K. R. Laurita, S. D. Girouard, F. G. Akar, and D. S. Rosenbaum, Circulation **98**, 2774 (1998).
[13] P. Comtois and A. Vinet, Chaos **12**, 903 (2002).
[14] B. Mensour, E. Jalil, A. Vinet, and T. Kus, Pacing Clin. Electrophysiol. **23**, 1200 (2000).
[15] A. Vinet, Ann. Biomed. Eng. **28**, 704 (2000).
[16] P. Comtois and A. Vinet, Phys. Rev. E **68**, 051903 (2003).
[17] B. Echebarria and A. Karma, Phys. Rev. Lett. **88**, 208101 (2002); E. Cytrynbaum and J. P. Keener, Chaos **12**, 788 (2002).
[18] E. M. Cherry and F. H. Fenton, Am. J. Physiol. **286**, H2332 (2004); $g(V,\vec{z})=I_{fi}+I_{so}+I_{si}$ where $I_{fi}=-vH(V-0.25)(V-0.15)\times(1-v)/0.15$, $I_{so}=V[1-H(V-0.16)]/1.5+H(V-0.16)/12.5$, $I_{si}=-0.5w\{1+\tanh[15(V-0.2)]\}/10$, and $H(V)$ is the Heaviside function. The time derivatives of the variables are $\partial_t v=[1-H(V-0.001)](1-v)/350-vH(V-0.25)/10$ and $\partial_t w=[1-H(V-0.25)](1-w)/48.5-wH(V-0.25)/562$.
[19] A plane wave is created at $x=0$ and premature excitations are initiated in the middle of the sheet. Since Neumann boundary conditions are applied, only one half of a sheet (10 by 6 cm) is simulated using an operator splitting and finite element method ($\Delta x=\Delta y=0.01$ cm and $\Delta t=0.01$ ms). Parameters in the model are $D=0.001$ cm^2/ms, and $I=0.3$, a finite square pulse of current used to initiate the normal wave and the PE. The PE are induced by localized stimuli applied on a square subset of nodes (29 by 15 nodes).
[20] F. Fenton and A. Karma, Phys. Rev. Lett. **81**, 481 (1998).
[21] M. Courtemanche, L. Glass, and J. P. Keener, Phys. Rev. Lett. **70**, 2182 (1993).
[22] M. Courtemanche, J. P. Keener, and L. Glass, SIAM J. Appl. Math. **56**, 119 (1996).
[23] This approximation on θ gives an upper limit for $\Delta_{b,R2}$ since the velocity decreases near the zone of the block and induces an increase in $T_{\mathrm{act},R2}$.
[24] P. Comtois, and A. Vinet, Phys. Rev. E **60**, 4619 (1999); Z. Qu, J. N. Weiss and A. Garfinkel, Am. J. Physiol. **276**, H269 (1999); F. Xie, Z. Qu, A. Garfinkel, and J. N. Weiss, *ibid.* **283**, H448 (2002).
[25] I. Banville and R. A. Gray, J. Cardiovasc. Electrophysiol. **13**, 1141–9 (2002).
[26] L. Priebe and D. J. Beuckelmann, Circ. Res. **82**, 1206 (1998).
[27] D. S. Ho *et al.*, J. Am. Coll. Cardiol. **22**, 1711 (1993).